INSTITUTE OF PHYSICS PUBLISHING JOURNAL OF PHYSICS: CONDENSED MATTER

J. Phys.: Condens. Matter **15** (2003) S709–S722 PII: S0953-8984(03)54547-7

The role of spin–orbit coupling in optically induced ultrafast magnetic dynamics*

R Gómez-Abal and W Hübner

Max-Planck-Institut für Mikrostrukturphysik, Weinberg 2, D-06120, Halle, Germany

E-mail: rgomez@mpi-halle.mpg.de

Received 9 October 2002
Published 27 January 2003
Online at stacks.iop.org/JPhysCM/15/S709

Abstract

Spin–orbit coupling (SOC) plays a major role in solid-state magnetism. Its effects range from completely defining the splitting of f states in rare earths to the correct prediction of the ground-state orientation of the magnetic moment in transition metals. The breaking of symmetries that it produces is the main tool for addressing magneto-optical effects. In this paper we theoretically study the possibility of all-optical spin switching. By simulating the effect of an ultrashort laser pulse on an electronic system, we show the crucial role of SOC in the spin dynamics occurring in this regime. The role of other parameters is also analysed. Finally, we show the possibility of obtaining an all-optical spin switching in the subpicosecond time regime.

1. Introduction

We are mainly interested in studying the possibility of all-optical spin switching. It is well known that for frequencies in the visible range and below, the wavelength is long enough that the electric dipole approximation for optical transitions is valid. Transitions of this kind are spin conserving. Thus, some non-spin-conserving interaction is needed to generate the spin dynamics.

Magneto-optical effects, such as Kerr and Faraday rotations, have been known of for a long time. As early as in 1932, Hulme [1] deduced that, for a ferromagnet, spin–orbit interaction of excited states was needed to produce magneto-optical effects. Later on, Argyres [2] showed that these effects originate from the combined action of spin–orbit coupling (SOC), exchange coupling, and the electric field of the light—SOC being not only important for its effect on the eigenenergies (as studied in [1]), but also in the wavefunctions.

The development of ultrashort laser pulses in the last few years, now as short as 5 to 15 fs, has opened up a whole new field of investigation [3–8]. Although so far predominantly applied to nonmagnetic solids, such as semiconductors and noble metals, for magnetic

* This paper is dedicated to Professor K Baberschke on the occasion of his 65th birthday.

0953-8984/03/050709+14$30.00

materials also the time-resolved (TR) spectroscopies such as the pump–probe magneto-optic Kerr effect (MOKE), two-photon photoemission (2PPE), and TR second-harmonic generation (SHG) approaches are now able to address a dynamical regime that had been considered as instantaneous.

Recent pump–probe experiments have shown a fast decay of the magneto-optical signal occurring on the subpicosecond timescale. The pioneering results of Beaurepaire *et al* [9] obtained by means of the TR MOKE for ferromagnetic Ni have indicated a decay of the magnetic signal by about 50% within about 1 ps. For $CoPt_3$, Beaurepaire *et al* [10] were able to achieve a complete disappearance of the magneto-optical signal within 500 fs. Later on, TR SHG experiments on Ni thin films by Hohlfeld *et al* [11] showed that the magnetic response can be faster than the electron thermalization, the latter being completed after 300 fs. 2PPE experiments performed by Scholl *et al* [12] showed two different demagnetization processes in Ni, on two different timescales. The first, instantaneous one was assigned to Stoner pair excitations, while the second, slower one, was attributed to spin–lattice relaxation processes taking place within 400 ps. Aeschlimann *et al* [13] found that the spin-resolved inelastic lifetimes of photo-excited electrons in Co are around 10 fs and are different for majority and minority spins.

More recently, experiments by Koopmans *et al* [14] on Ni provided evidence for a state-filling effect (bleaching) visible in the TR MOKE during the very first instants of the dynamics, followed by a true demagnetization after about 200 fs. TR SHG measurements by Regensburger *et al* [15] led them to the conclusion that TR SHG is not necessarily the signature of magnetization dynamics. Guidoni *et al* [16] found recently, for $CoPt_3$ alloys, that an ultrafast spin dynamics occurs during the thermalization of the electronic populations with a characteristic time of about 50 fs, followed by a quasistatic equilibrium where the spins follow the dynamics of the electronic temperature.

Previous theoretical works have successfully taken a first step towards disentangling the dynamical processes taking place on the various timescales:

(i) 'bleaching' (blocking of the response to the probe pulse by state filling, 1 fs) [17];

(ii) magnetic dephasing (electron spin relaxation, a few femtoseconds) [17];

(iii) genuine demagnetization, (20–40 fs) [18];

(iv) spin–lattice relaxation (304 ps for Ni) [17].

It is important to notice that the processes (iii) and (iv) rely on SOC while (i) and (ii) do not.

These exciting results demonstrated a considerable amount of control of the magnetic dynamics by an appropriate choice of the laser pulse parameters (central pulse frequency, amplitude, pulse duration) for metallic Ni, but failed to obtain a controlled *switching* of the magnetic moment[1]. This is due to the fact that the electrons are excited into dispersive bands, in which the coherence is lost very quickly and control is impossible. Thus it is better to use systems with discrete levels, such as nanoparticles, or gap states in insulators. The latter are present in NiO, which is a charge transfer insulator, having a gap of 4.4 eV and magnetic moment of 1.9 μ_B per Ni atom [19]. Its multiplet states within the gap seem to offer a good scenario for this controlled dynamics.

[1] Note that switching of a quantum spin state involves its destruction, unlike the coherent rotation of a classical magnetization vector by a perpendicularly applied magnetic field pulse.

2. Theory

The general statement of a quantum dynamical problem can be usually described with a model Hamiltonian that has the form

$$\hat{H}(x,t) = \hat{H}_0(x) + \hat{V}(x,t) \tag{1}$$

where it is possible to separate the time-independent part (H_0) from the time-dependent one ($V(x,t)$). As usual, the basis functions used to solve such a problem are the eigenfunctions of the time-independent Hamiltonian (H_0). In our case, the time-independent Hamiltonian corresponds to the solution of the electronic structure of the system that we want to study, while $V(x,t)$ is the interaction of the electronic system with the electromagnetic field of the laser. Since the frequencies of interest are in the visible range, corresponding to wavelengths of the order of hundred of nanometres, the spatial dependence of the vector potential can be neglected. This corresponds to making the electric dipolar approximation, in which this term has the form

$$\hat{V}(x,t) = \hat{V}(t) = e\hat{\boldsymbol{r}} \cdot \boldsymbol{E}(t) \tag{2}$$

where $e\hat{\boldsymbol{r}}$ is the electric dipole moment operator and $\boldsymbol{E}(t)$ is the electric field of the laser, whose time dependence is given by

$$\boldsymbol{E}(t) = \boldsymbol{E}_0 \exp\left[-\left(\frac{t}{\tau}\right)^2 - \mathrm{i}\omega_0 t\right]. \tag{3}$$

Since we are interested in the response of the system to the application of several laser pulses and, experimentally, these pulses are not isolated but periodically repeated, we simulate the laser by a periodically applied pulse.

This periodicity allows one to use numerical methods specially designed for such cases. One of these is the Floquet method, which consists of a transformation of the time periodic problem to the frequency space, similarly to the Bloch theorem in space periodic problems in the solid state. A detailed explanation of the theory, as well as the Floquet-matrix method, is given in the appendix. Unfortunately, the method has proved to be quite inefficient in application in the cases we are interested in, due to the large number of harmonics needed to describe simultaneously and on the same footing pulses whose main frequency and width are in the femtosecond range and a modulation period of the order of several nanoseconds [20].

Instead, we have used a direct time integration method in one period [21] to solve the time-dependent Schrödinger equation

$$\hat{H}(x,t)\psi(x,t) = \mathrm{i}\hbar\,\frac{\partial}{\partial t}\psi(x,t). \tag{4}$$

The quantum states evolve in time according to

$$\psi(t) = \hat{U}(t,0)\psi(0) \tag{5}$$

where $\hat{U}(t,0)$ is the time evolution operator, obeying the equation

$$\frac{\mathrm{d}}{\mathrm{d}t}\hat{U}(t,0) = -\frac{\mathrm{i}}{\hbar}\hat{H}(t)\hat{U}(t,0). \tag{6}$$

The time evolution of any observable as a function of time is given by

$$\langle\hat{Q}(t)\rangle = \mathrm{Tr}(\hat{\rho}(t)\hat{Q}) = \mathrm{Tr}(\hat{U}(t,0)\hat{\rho}(0)\hat{U}^{\dagger}(t,0)\hat{Q}). \tag{7}$$

Thus, to solve for the evolution of a quantum system it is sufficient to know its time evolution operator $\hat{U}(t,0)$. To calculate this operator we follow the method explained in [20].

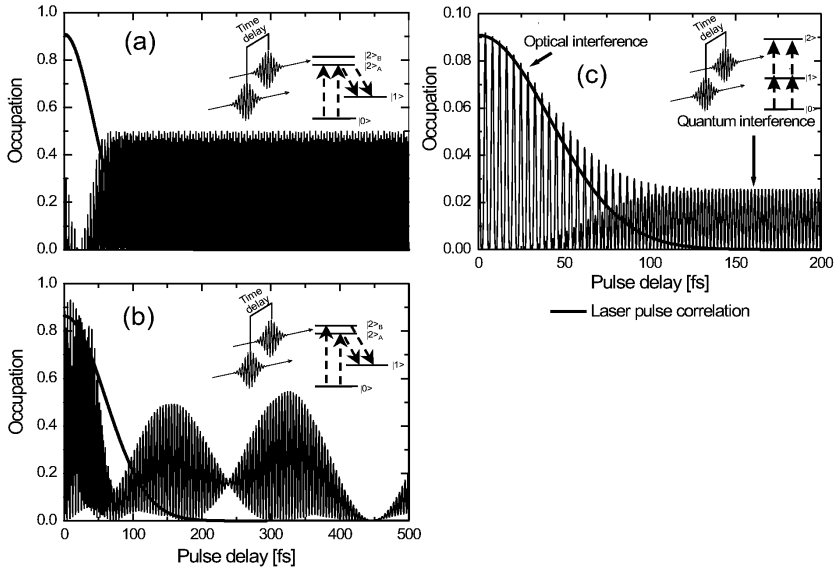

Figure 1. (a) Occupation of state $|1\rangle$ as a function of the time delay between the pulses, when the two laser pulses are tuned to the state $|2\rangle_A$. (b) Occupation of state $|1\rangle$ when one of the pulses is tuned to state $|2\rangle_A$ and the other to state $|2\rangle_B$. (c) Occupation of state $|2\rangle$ when the two pulses are tuned to half the $|0\rangle \rightarrow |2\rangle$ energy difference, but slightly detuned from the transition $|0\rangle \rightarrow |1\rangle$.

3. Results

3.1. Charge dynamics: coherent control; quantum and optical interference

Coherent control of electron dynamics is a well developed field in semiconductor physics. As a test calculation, we show our ability to qualitatively reproduce some experimental results obtained in the field, regarding quantum interference. Afterwards we transfer these ideas to the control of magnetism.

As a first test we consider the experiments by Bonadeo *et al* [22] on GaAs quantum dots. The level scheme addressed in the experiment consists of the four levels shown in the inset of figures 1(a) and (b). The laser pulses excite electrons from the ground state ($|0\rangle$) to any of the states $|2\rangle_A$ and $|2\rangle_B$. These states decay very fast to the intermediate state ($|1\rangle$), and the light emission due to the decay $|1\rangle \rightarrow |0\rangle$ is then measured as a function of the time delay between the pulses. Since the decay from any of the states $|2\rangle_A$ and $|2\rangle_B$ to state $|1\rangle$ is much faster than any other process, we can consider it as instantaneous. This means that at each time step, the wavefunction of this state is the one corresponding to the sum of the wavefunctions of the levels $|2\rangle_A$ and $|2\rangle_B$, effectively reducing our calculation to a three-level system. Whether a given laser pulse excites the electrons from the ground state to the $|2\rangle_A$ or $|2\rangle_B$ levels depends, experimentally, not only on the main frequency of the pulse but also on its polarization, due to different selection rules resulting from the different symmetries of the states. In our calculation, this effect is simulated by turning on and off the corresponding matrix element $\langle 0|V(t)|2\rangle$. Since our model does not include any decay mechanism for state $|1\rangle$ we calculate its occupation in the asymptotic limit, i.e. a long time after the second pulse has been applied. Figure 1 displays the occupation obtained in this way as a function of the delay between the two pulses.

When both laser pulses are tuned to resonance with the transition to state $|2\rangle_A$, and with the corresponding polarization, the result obtained is that shown in figure 1(a). The results

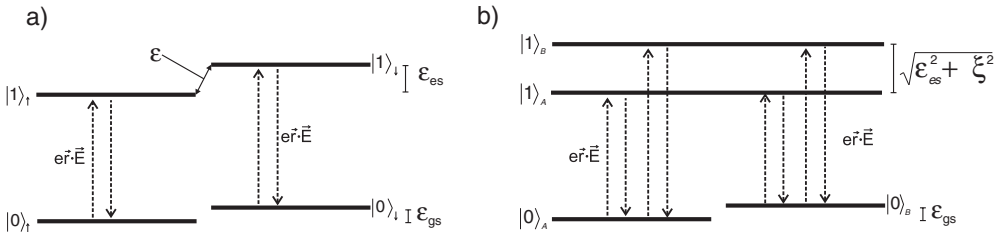

Figure 2. The minimum level scheme for optically induced spin dynamics.

also show the oscillatory regime that extends far beyond the pulse correlation, showing that this is a quantum interference effect, as found experimentally [22].

When the second pulse is tuned to resonance with the transition from level $|0\rangle$ to $|2\rangle_B$ (figure 1(b)) the oscillations due to interference as well as the beatings due to the slightly different energies can be clearly observed.

The distinction between optical and quantum interference was observed experimentally for the first time by Blanchet *et al* [23] in the two-photon excitation to the $7d\ ^2D_{3/2,5/2}$ fine-structure doublet in Cs. Using a three-level system, where the levels are at 0.0, 0.9, and 2.0 eV (inset of figure 1(c)), exciting the system with two identical pulses with their main photon frequency corresponding to 1 eV, we are able to clearly see the distinction between the two kinds of interference and the transition between them (figure 1(c)) due to the frequency doubling in the time dependence of the occupation. Thus, our three-level model system correctly describes different charge dynamics phenomena. It yields quantum interference and can distinguish it from the optical interference between the laser pulses.

3.2. Optically induced spin dynamics I: a simple model

What we have shown so far is coherent control of electron dynamics and the distinction between quantum and optical interference, but the spin of the electrons has not yet been included. In a previous work [20] we have shown the possibility of switching between two degenerate electronic ground states via an optical excitation to a high-lying state and back. The transition was complete if the central frequency of the laser was resonant with the level splitting and the width of the pulse was tuned according to its intensity. Such a system should constitute a perfect quantum bit, if there is some symmetry property which can distinguish the two levels and can be measured. For that property to be the spin of the electron, it is necessary that the excited state is a spin mixed state, otherwise one of the transitions should not be allowed.

To obtain a spin mixed state, two excited states of definite (and opposite) spin are needed, which are mixed through SOC. Thus, the minimum scenario for optically induced spin dynamics (and therefore for all-optical spin switching) is a four-level system as shown in figure 2.

Comparison of this system with the one of figure 7 in [20] show that three new parameters enter into play, namely

(i) the splitting of the two lower states, which could be due to Zeeman splitting, gyromagnetic energies, or magnetic anisotropy barriers (ε_{gs} where subscript gs indicates the ground state);
(ii) the splitting of the two higher states, which could be due to the same factors as mentioned in (i) or to the symmetries of the system (ε_{es} where subscript es indicates the excited state);
(iii) the strength of the SOC (ξ).

In the following we will analyse the role of each of them in the spin dynamics. The matrix representing the Hamiltonian in this model, using the pure spin states as a basis, can be written as

$$\overline{H}_0 = \begin{pmatrix} E_0 & 0 & 0 & 0 \\ 0 & E_0 + \varepsilon_{gs} & 0 & 0 \\ 0 & 0 & E_1 & \xi/2 \\ 0 & 0 & \xi/2 & E_1 + \varepsilon_{es} \end{pmatrix}. \tag{8}$$

The eigenvalues of this Hamiltonian are

$$\varepsilon_{0\uparrow} = E_0, \qquad \varepsilon_{0\downarrow} = E_0 + \varepsilon_{gs} \tag{9a}$$

$$\varepsilon_{1A} = E_1 + \frac{\varepsilon_{es}}{2} - \frac{1}{2}\sqrt{\varepsilon_{es}^2 + \xi^2}, \qquad \varepsilon_{1B} = E_1 + \frac{\varepsilon_{es}}{2} + \frac{1}{2}\sqrt{\varepsilon_{es}^2 + \xi^2} \tag{9b}$$

and the corresponding eigenvectors are

$$|0\rangle_A = |0\rangle_\uparrow, \qquad |0\rangle_B = |0\rangle_\downarrow \tag{10a}$$

$$|1\rangle_A = \frac{1}{\sqrt{2}} \frac{\xi}{\sqrt{\varepsilon_{es}^2 + \xi^2 - \varepsilon_{es}\sqrt{\varepsilon_{es}^2 + \xi^2}}} |1\rangle_\uparrow + \frac{1}{\sqrt{2}} \frac{\varepsilon_{es} - \sqrt{\varepsilon_{es}^2 + \xi^2}}{\sqrt{\varepsilon_{es}^2 + \xi^2 - \varepsilon_{es}\sqrt{\varepsilon_{es}^2 + \xi^2}}} |1\rangle_\downarrow \tag{10b}$$

$$|1\rangle_B = \frac{1}{\sqrt{2}} \frac{\xi}{\sqrt{\varepsilon_{es}^2 + \xi^2 + \varepsilon_{es}\sqrt{\varepsilon_{es}^2 + \xi^2}}} |1\rangle_\uparrow + \frac{1}{\sqrt{2}} \frac{\varepsilon_{es} + \sqrt{\varepsilon_{es}^2 + \xi^2}}{\sqrt{\varepsilon_{es}^2 + \xi^2 + \varepsilon_{es}\sqrt{\varepsilon_{es}^2 + \xi^2}}} |1\rangle_\downarrow. \tag{10c}$$

In the limiting cases, for $\xi = 0$ the Hamiltonian is already diagonal and no spin dynamics can be observed. In the limit where $\varepsilon_{es} = 0$ the excited state eigenvalues reduce to

$$\varepsilon_{1A} = E_1 - \frac{|\xi|}{2}, \qquad \varepsilon_{1B} = E_1 + \frac{|\xi|}{2} \tag{11}$$

with the corresponding eigenvectors

$$|1\rangle_A = \frac{1}{\sqrt{2}}(|1\rangle_\uparrow - |1\rangle_\downarrow), \qquad |1\rangle_B = \frac{1}{\sqrt{2}}(|1\rangle_\uparrow + |1\rangle_\downarrow) \tag{12}$$

constituting the best scenario for spin switching: the larger the SOC parameter, the better, since then ε_{1B} is far enough away in energy to be out of resonance and we are back in the three-level system. Here, the excited state has a probability of $\frac{1}{2}$ for each spin.

Taking this limit ($\varepsilon_{es} = 0$), and with realistic orders of magnitude for the Zeeman splitting ($\varepsilon_{gs} = 1$ meV) and the SOC parameter ($\xi = 0.1$ eV), we were able to obtain spin switching within a few femtoseconds, as can be seen in figure 3.

To analyse the dependence of the dynamics with the parameters previously mentioned, we will start with the splitting within the two levels $|0\rangle_\uparrow$ and $|0\rangle_\downarrow$. In this case one question arises immediately: to obtain a complete transition, both states must be in resonance with the higher one; once the two lower states are not degenerate, what frequency should we choose? In figure 4 we show two cases. In the first one, we choose the central frequency of the laser pulse such that state $|0\rangle_\uparrow$ is resonant with state $|1\rangle_A$. In this case the state $|0\rangle_\uparrow$ will be out of resonance at some value of ε_0, and that transition will not happen any longer. The other possibility is to choose the main frequency of the laser to be the mean between the resonances corresponding to the transitions $|0\rangle_\uparrow \rightleftarrows |1\rangle_A$ and $|0\rangle_\downarrow \rightleftarrows |1\rangle_A$. The results show that the splitting of these levels can completely avoid the switching of the spins for values larger than 0.08 eV. Of course, this value is not general, and is determined by the spectral width of the pulse. For smaller values, the selection of the central frequency of the laser is not important. For larger values, choosing the central frequency resonant with the $|0\rangle_\uparrow \rightleftarrows |1\rangle_A$ transition is more efficient.

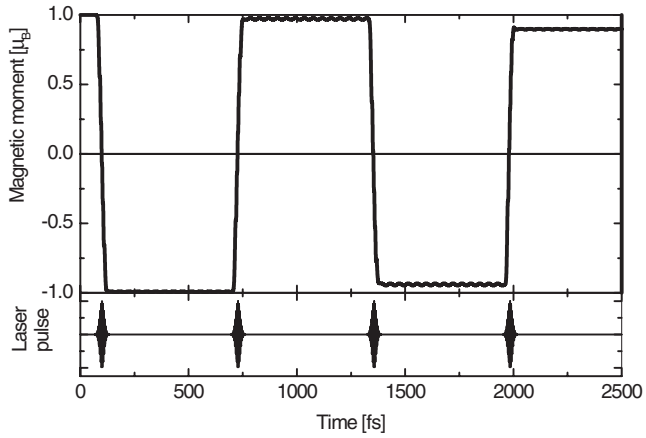

Figure 3. The instantaneous value of the magnetic moment as a function of time in the four-level system.

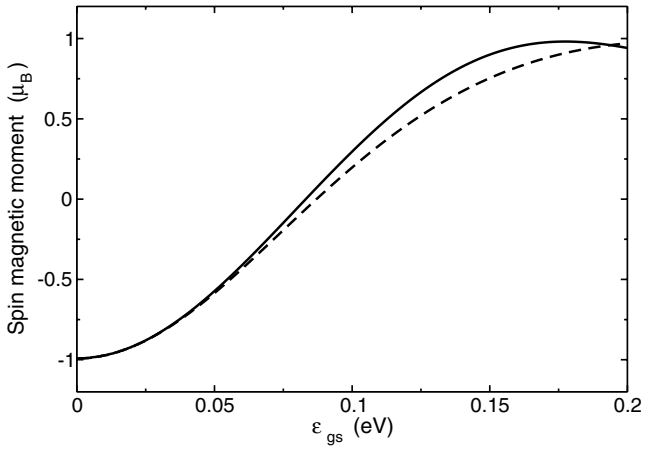

Figure 4. Spin magnetic moment after the application of a laser pulse as a function of the *Zeeman splitting* in the four-level system: for the central frequency of the pulse lying between the resonances corresponding to the transitions $|0\rangle_\uparrow \rightleftarrows |1\rangle_A$ and $|0\rangle_\downarrow \rightleftarrows |1\rangle_A$ (full curve) and when it is resonant with $|0\rangle_\uparrow \rightleftarrows |1\rangle_A$ (dashed curve).

Making shorter pulses should keep the two levels $|0\rangle_A$ and $|0\rangle_B$ in resonance for a larger range of values for ε_{gs}, since the frequency width of the pulse increases. On the other hand, pulses wider in energy will also be in resonance with level $|1\rangle_B$, which is not desirable since the interference between the two excited states works against the control of the populations.

As regards the dependence with the other two parameters (ε_{es} and ξ), we have already seen the limiting cases. We saw already that SOC is indispensable for optically inducing spin dynamics. Figure 5 shows the dependence of the spin magnetic moment (shading) on both the pulse duration, measured by its temporal full width at half-maximum (FWHM) (y-axis), and the SOC parameter (ξ) (x-axis). The parameter E_1 is varied such that the position of the level $|1\rangle_A$ is fixed at 1 eV, and ε_{es} is set equal to zero. The behaviour is clear: the larger the SOC, the shorter the pulses needed to obtain complete spin switching. In other words, as ξ increases, the state $|1\rangle_B$ gets higher in energy, the system gets closer to the three-level system, and the laser gets more efficient at performing the switching.

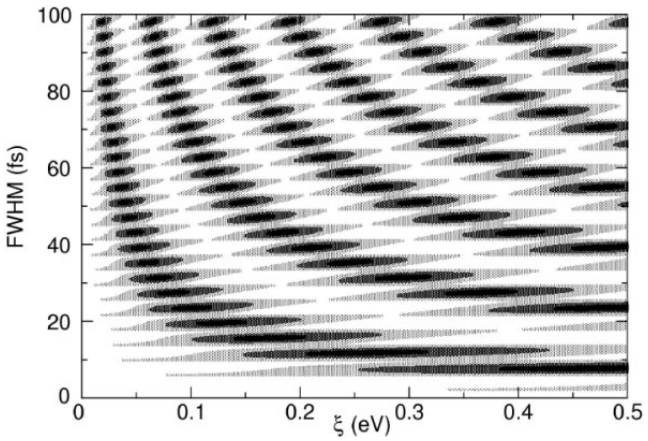

Figure 5. The dependence of the spin magnetic moment (μ) (shading) after the application of the laser pulse on both the pulse duration, measured by its temporal FWHM (y-axis), and the SOC parameter (ξ) (x-axis). Black areas correspond to μ lower than -0.9, dark grey to μ between -0.9 and -0.5, light grey to μ between -0.5 and 0.0, and white areas to positive values of μ.

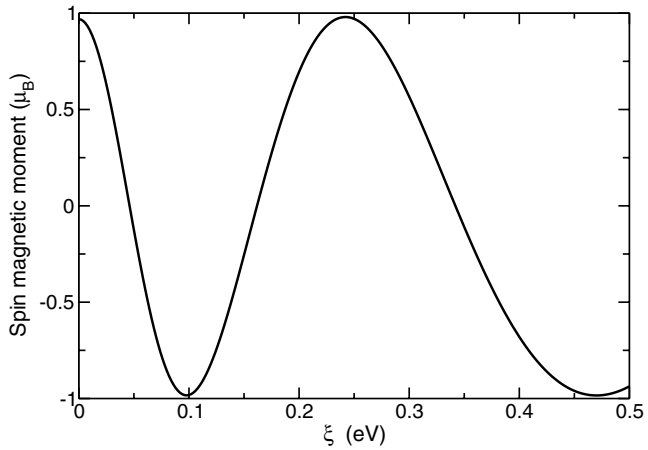

Figure 6. The dependence of the spin magnetic moment (μ) after the application of the laser pulse on the SOC parameter (ξ) for FWHM $= 19.4$ fs.

In figure 6 we show the dependence of the spin magnetic moment (μ) on the SOC parameter (ξ) for a pulse of FWHM $= 19.4$ fs—that is, taking a horizontal line in figure 5 at that value on the y-axis.

It is interesting to compare the role of ξ with that of ε_{es} by comparing the behaviours of μ in figures 6 and 7. The latter shows the dependence of μ on the parameter ε_{es} for $\xi = 0.1$ eV and different pulse durations. While, at first sight, the results look similar, especially for small values of ε_{es}, the reason for such a behaviour is very different. While in figure 6 the spin is not reversed due to the fact that the pulse is too long and the transition starts to come back, in figure 7 the effect is due to a slowing down of the switching, due to the smaller mixing of the spins for higher-lying excited states (keeping ξ constant). That can be clearly seen from the fact that there are no oscillations and, for values of ε_{es} that are big enough, there is no spin dynamics at all.

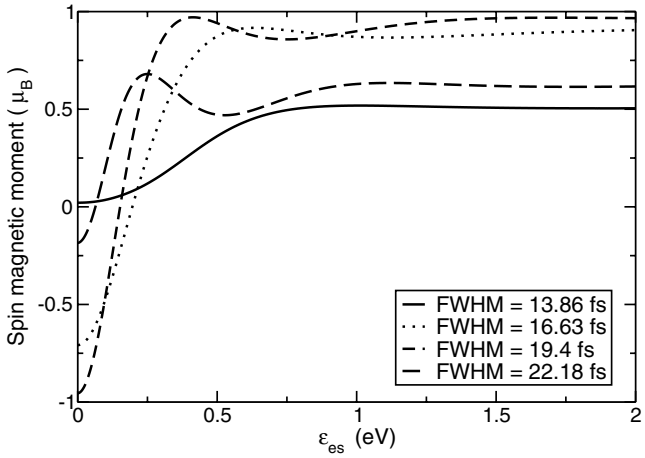

Figure 7. The dependence of the spin magnetic moment (μ) after the application of the laser pulse on the parameter ε_{es} for $\xi = 0.1$ eV and different pulse durations.

Up to now we have studied the conditions for an all-optical spin switching and the role played by spin–orbit and other characteristics of the electronic system in the simple four-level model. The next step is to include a realistic description of a material where such conditions could be fulfilled.

3.3. Optically induced spin dynamics II: NiO

As we have already mentioned in the introduction, multiplet states within the gap of the NiO(001) surface seem to provide a good scenario for optically induced spin dynamics.

The energies and wavefunctions of the multiplet states were obtained by fitting a ligand field theory, which exploits the symmetry of the system, to the low-lying states obtained experimentally [24]. This allows us to extend the results to the whole set of two-hole multiplet levels in NiO, both for the (001) surface (C_{4v} symmetry) and the bulk (O_h symmetry), as can be seen in figure 8 (data from [25]).

For the SOC parameter we have used the value $\xi = 0.1$ eV. The time-dependent part corresponds to the interaction with the laser electric field given by (2) and (3). For the electric dipole ($e\hat{\boldsymbol{r}}$) matrix elements, we used the values of [26].

We take a circularly polarized laser pulse in order to make it work also as an angular momentum reservoir. The main frequency of the laser is chosen to be in resonance with some excited levels, as shown in figure 2 and in [20]. Several possibilities appear with the NiO levels; the first excited states are the ^{3}E levels in figure 8, which, in the presence of SOC, are split into five different states with energies between 0.62 and 0.7 eV. After trying many frequencies around this interval, a 'best' result was obtained, and this is shown in figure 9, with a main frequency $\hbar\omega_0 = 0.675$ eV and a FWHM of the laser pulse of 114 fs. The result does not depend on the time delay between pulses. Shorter pulses would not give a better result, since they should be wider in the frequency space, exciting many of the exited states ^{3}E simultaneously, thus making the control of the dynamics impossible.

Another option is to excite the system to the levels of NiO around 1.5 eV, which lies in the visible range and could easily be addressed by experiments. This also corresponds to states of ^{3}E symmetry, where the same kind of transition is allowed. The splitting of the states due to SOC is of the same order. Thus, a similar result is obtained, as shown in figure 10, for the

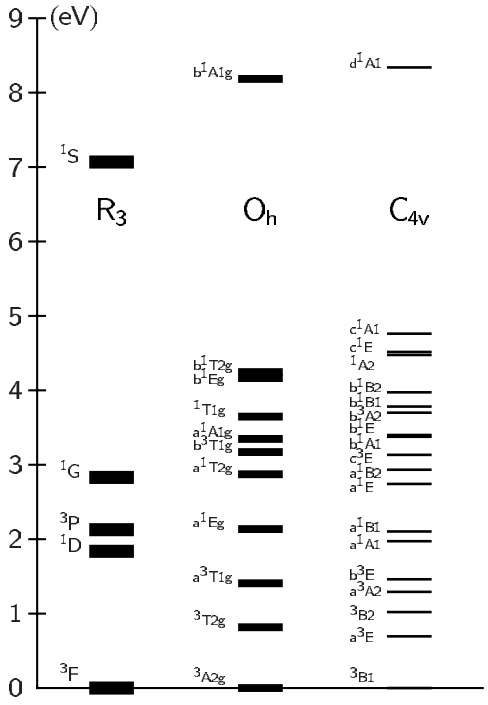

Figure 8. The level scheme of the NiO gap states obtained from the ligand field theory fitted to experiments (from [25]).

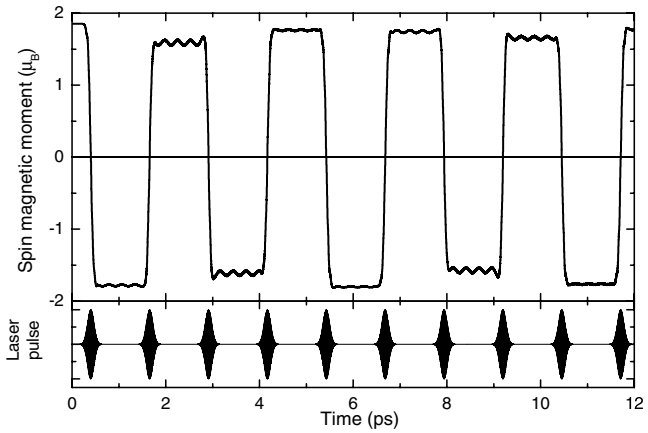

Figure 9. Magnetic moment as a function of time for NiO(001). For the parameters of the laser pulse see the text.

central laser frequency of $1.425\frac{\text{eV}}{\hbar}$ in resonance with the energy of the excited state involved. These figures demonstrate a complete spin switching within 200 fs, which can be maintained for more than ten duty cycles.

It can be observed from our calculations that the state lasts for more than 10 ps. Our model does not include phonons as a source of dephasing. Their inclusion might even improve our results, since once the 'barrier' has been crossed, the phonons make the system decay to the

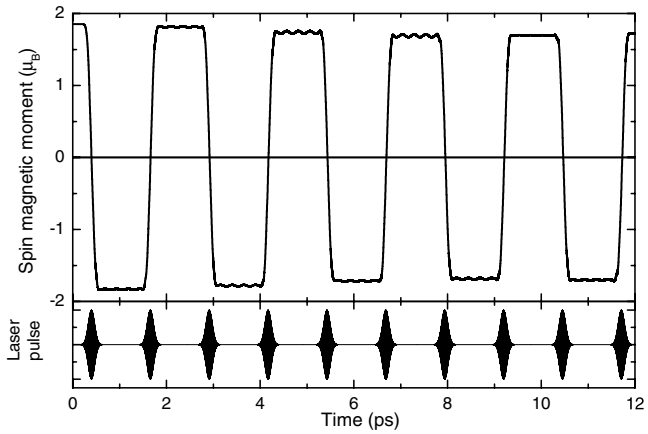

Figure 10. Magnetic moment as a function of time for NiO(001) excited with a $\lambda = 870$ nm laser pulse. Central frequency $1.425\,\frac{\mathrm{eV}}{\hbar}$, FWHM $= 111$ fs, fluence $\approx 1.4 \times 10^{14}\,\frac{\mathrm{W}}{\mathrm{cm}^2}$.

completely switched state. This should take times of the order of the nanoseconds. This will improve also the number of duty cycles, since the switching will be complete, then constituting a new start for what we have shown in figure 10.

4. Conclusions

Through the sections of this paper we have shown that ultrafast optically induced spin dynamics is only possible in the presence of SOC. We have described an efficient method for the computation of the dynamics of an electronic system during and after the application of one or more laser pulses. Revisiting experimental results, we tested the capability of this calculation of addressing charge dynamics and interference effects within it. We could clearly distinguish between quantum and optical interference.

The simplest scenario for optically induced spin dynamics has been shown. It consists of a four-level system: two almost degenerate pure spin states at low energy and two also almost degenerate states at high energy which can be mixed by SOC. The role of SOC has been shown to be crucial. Other interactions that could break the degeneracies of the states, such as the Zeeman effect and gyromagnetic energies, are counterproductive for the optically induced spin dynamics.

Finally, we have identified NiO as a system in which such a scenario is given. The possibility of obtaining a complete spin switching on subpicosecond timescales is demonstrated; this is much faster than anything found up to now.

Acknowledgments

We acknowledge the support of DFG through SFB 418 and FG 404, and by the EU research training networks DYNAMICS and EXCITING.

Appendix. Floquet theory

As was stated in section 2, we are interested in solving the Schrödinger equation for periodically repeated pulse trains. That means that the Hamiltonian will be a periodic function of time,

i.e. $H(t) = H(t+\tau)$. In particular, if we call $V(\vec{r},t)$ the time-dependent perturbation, then the Schrödinger equation for the quantum system can be written as

$$\left(H(\vec{r},t) - \mathrm{i}\hbar\frac{\partial}{\partial t}\right)\Psi(\vec{r},t) = 0 \tag{A.1}$$

with $H(\vec{r},t) = H_0(\vec{r}) + V(\vec{r},t)$, $V(\vec{r},t) = V(\vec{r},t+\tau)$.

The unperturbed Hamiltonian $H_0(\vec{r})$ is assumed to possess a complete orthonormal set of eigenfunctions $\phi_n(\vec{r})$ with corresponding eigenvalues E_n. According to the Floquet theorem, there exist solutions to (A.1) that have the form

$$\Psi_\alpha(\vec{r},t) = \exp\left(-\mathrm{i}\frac{\varepsilon_\alpha t}{\hbar}\right)\Phi_\alpha(\vec{r},t), \tag{A.2}$$

which is the so-called Floquet-state solution and where $\Phi_\alpha(\vec{r},t)$ is a Floquet mode obeying

$$\Phi_\alpha(\vec{r},t) = \Phi_\alpha(\vec{r},t+\tau). \tag{A.3}$$

The parameter ε_α is real and unique up to multiples of $\hbar\omega$, $\omega = \frac{2\pi}{\tau}$. It is called the Floquet characteristic exponent, or quasienergy. One can see the formal analogy between the Floquet theorem in the time–energy regime and the Bloch theorem in the space–momentum regime, which is reflected in the term quasienergy, analogously to the term quasimomentum ($\vec{k}$) characterizing the Bloch eigenstates in a periodic solid.

Upon substituting (A.2) into (A.1) one obtains the eigenvalue equation for the quasienergy ε_α:

$$\mathcal{H}(\vec{r},t)\Phi_\alpha((\vec{r},t) = \varepsilon_\alpha\Phi_\alpha(\vec{r},t), \qquad \text{with } \mathcal{H}(\vec{r},t) \equiv H(\vec{r},t) - \mathrm{i}\hbar\frac{\partial}{\partial t}. \tag{A.4}$$

It can be immediately noticed that the Floquet modes

$$\Phi_{\alpha'}(\vec{r},t) = \Phi_\alpha(\vec{r},t)\exp(\mathrm{i}p\omega t) \equiv \Phi_{\alpha p}(\vec{r},t) \tag{A.5}$$

with n being an integer number ($p = 0, \pm1, \pm2, \ldots$) yield an identical solution to that in (A.2), but with the shifted quasienergy

$$\varepsilon_\alpha \to \varepsilon_{\alpha'} = \varepsilon_\alpha + p\hbar\omega \equiv \varepsilon_{\alpha p}. \tag{A.6}$$

Hence, the index α corresponds to a whole class of solutions labelled by subscripts $\alpha' = (\alpha, p)$, $p = 0, \pm1, \pm2, \ldots$. The eigenvalues ε_α can be mapped into a *first Brillouin zone*, defined by the interval $-\frac{\hbar\omega}{2} \leqslant \varepsilon < \frac{\hbar\omega}{2}$. A more detailed description of the general properties of Floquet theory can be found in [27].

A.1. Floquet-matrix method

Since exactly solvable quantum systems with an explicitly time-dependent interaction potential are extremely rare, one generally has to invoke numerical procedures. In the case of Floquet theory, one of them is the Floquet-matrix method. It makes use of the fact that the Hamiltonian $H(\vec{r},t)$ and the Floquet modes are time periodic, equation (A.3). Therefore we can expand the Floquet solutions ($\Phi_\alpha(\vec{r},t)$) into the Fourier vectors $|n\rangle$, $n = 0, \pm1, \pm2, \ldots$ such that $\langle t|n\rangle = \exp(\mathrm{i}n\omega t)$. Then,

$$\Phi_\alpha(\vec{r},t) = \sum_{n=-\infty}^{\infty} c_\alpha^n(\vec{r})\exp(\mathrm{i}n\omega t). \tag{A.7}$$

The functions $c_\alpha^n(\vec{r})$ can be expanded in terms of the eigenfunctions $\{\phi_k(\vec{r}), k = 1, \ldots, \infty\}$ of the unperturbed Hamiltonian $H_0(\vec{r})$:

$$\Phi_\alpha(\vec{r},t) = \sum_{k=1}^{\infty}\sum_{n=-\infty}^{\infty} c_{\alpha,k}^n\phi_k(\vec{r})\exp(\mathrm{i}n\omega t), \tag{A.8}$$

with $c^n_{\alpha,k} = \langle\phi_k|c^n_\alpha\rangle$. Hence, in terms of the kets $\{|\phi_k\rangle, \langle\vec{r}|\phi_k\rangle = \phi_k(\vec{r})\}$, the Floquet equation (A.4) reads

$$\sum_{k=1}^{\infty}\sum_{n=-\infty}^{\infty}\mathcal{H}c^n_{\alpha,k}|\phi_k\rangle\exp(\mathrm{i}n\omega t) = \sum_{k=1}^{\infty}\sum_{n=-\infty}^{\infty}\varepsilon_\alpha c^n_{\alpha,k}|\phi_k\rangle\exp(\mathrm{i}n\omega t). \tag{A.9}$$

Setting $\langle\phi_k|\langle m| \equiv \langle\phi_k m|$, multiplying (A.9) by $\langle\phi_j m|\exp(-\mathrm{i}m\omega t)$ from the left, and averaging over one time period of driving, the system of equations becomes

$$\sum_{n=-\infty}^{\infty}\sum_{k=1}^{\infty}\langle\langle\phi_j m|\mathcal{H}|\phi_k n\rangle\rangle c^n_{\alpha,k} = \varepsilon_\alpha c^n_{\alpha,j}. \tag{A.10}$$

where we have used the shorthand notation

$$\langle\langle\Phi_\alpha|\mathcal{H}|\Phi_\beta\rangle\rangle \equiv \frac{1}{\tau}\int_0^\tau\langle\Phi_\alpha|\mathcal{H}|\Phi_\beta\rangle(t)\,\mathrm{d}t \tag{A.11}$$

with

$$\langle\Phi_\alpha|\mathcal{H}|\Phi_\beta\rangle(t) \equiv \iiint_{-\infty}^{\infty}\Phi^*_\alpha(\vec{r},t)\mathcal{H}(\vec{r},t)\Phi_\beta(\vec{r},t)\,\mathrm{d}\vec{r}. \tag{A.12}$$

Defining

$$H^{m-n} = \frac{1}{\tau}\int_0^\tau H(t)\exp[-\mathrm{i}(m-n)\omega t]\,\mathrm{d}t, \tag{A.13}$$

one finds the Floquet-matrix representation for (A.9):

$$\sum_{n=-\infty}^{\infty}\sum_{k=1}^{\infty}\langle\langle\phi_j m|\mathcal{H}_F|\phi_k n\rangle\rangle c^n_{\alpha,k} = \varepsilon_\alpha c^n_{\alpha,j}. \tag{A.14}$$

with the Floquet matrix defined by

$$\langle\langle\phi_j m|\mathcal{H}_F|\phi_k n\rangle\rangle \equiv \langle\phi_j|H^{m-n}|\phi_k\rangle + n\hbar\omega\delta_{n,m}\delta_{j,k}. \tag{A.15}$$

The quasienergies ε_α are now obtained as the eigenvalues of the secular equation

$$\det[\mathcal{H}_F - \varepsilon\mathbb{I}] = 0. \tag{A.16}$$

by providing the quasienergies $\varepsilon_{\alpha,n}$ and their corresponding eigenvectors $|\varepsilon_{\alpha,n}\rangle$, which obey the already mentioned periodicity properties

$$\varepsilon_{\alpha,k} = \varepsilon_{\alpha,0} + k\hbar\omega, \qquad \langle\alpha, n+k|\beta, m+k\rangle = \langle\alpha, n|\beta, m\rangle. \tag{A.17}$$

Once the eigenvalues and eigenstates of the system are obtained, the full time evolution of the system can be described. Thus just one diagonalization, namely that of $\mathcal{H}_F$, suffices; the disadvantage is that $\mathcal{H}_F$ is an infinite matrix, which must be truncated at some point. The efficiency of the method has been analysed in [20].

References

[1] Hulme H R 1932 *Proc. R. Soc.* A **135** 237–57
[2] Argyres P N 1955 *Phys. Rev.* **97** 334–45
[3] Fann W S, Storz R, Tom H W K and Bokor J 1992 *Phys. Rev. Lett.* **68** 2834
[4] Hertel T, Knoesel E, Wolf M and Ertl G 1996 *Phys. Rev. Lett.* **76** 535
[5] Höfer U, Shumay I L, Thomann U, Wallauer W and Fauster T 1998 *Science* **279** 190
[6] Tom H W K, Chang Y M and Kwak H 1999 *Appl. Phys.* B **68** 305
[7] Bigot J Y, Halté V, Merle J C and Daunois A 2000 *Chem. Phys.* **251** 181
[8] Lamprecht N, Schider G, Lechner R T, Ditlbacher H, Krenn J, Leitner A and Aussenegg F R 2000 *Phys. Rev. Lett.* **84** 4721

[9] Beaurepaire E, Merle J C, Daunois A and Bigot J Y 1996 *Phys. Rev. Lett.* **76** 4205
[10] Beaurepaire E, Maret M and Halté V 1998 *Phys. Rev.* B **58** 12134
[11] Hohlfeld J, Matthias E, Knorren R and Bennemann K H 1997 *Phys. Rev. Lett.* **78** 4861
[12] Scholl A, Baumgarten L, Jacquemin R and Eberhardt W 1997 *Phys. Rev. Lett.* **79** 5146
[13] Aeschlimann M, Bauer M, Pawlik S, Weber W, Burgermeister R, Oberli D and Siegmann H C 1997 *Phys. Rev. Lett.* **79** 5158
[14] Koopmans B, van Kampen M, Kohlhepp J T and de Jonge W J M 2000 *Phys. Rev. Lett.* **85** 844
[15] Regensburger H, Vollmer R and Kirschner J 2000 *Phys. Rev.* B **61** 14716
[16] Guidoni L, Beaurepaire E and Bigot J Y 2002 *Phys. Rev. Lett.* **89** 017401
[17] Hübner W and Zhang G P 1998 *Phys. Rev.* B **58** R5920
[18] Zhang G P and Hübner W 2000 *Phys. Rev. Lett.* **85** 3025
[19] Cheetham A K and Hope D A 1983 *Phys. Rev.* B **27** 6964
[20] Gómez-Abal R and Hübner W 2002 *Phys. Rev.* B **65** 195114
[21] Edén M, Lee Y K and Levitt M 1996 *J. Magn. Reson.* A **120** 56
[22] Bonadeo N H, Erland J, Gammon D, Park D, Katzer D S and Steel D G 1998 *Science* **282** 1473–6
[23] Blanchet V, Nicole C, Bouchene M A and Girard B 1997 *Phys. Rev. Lett.* **78** 2716
[24] Fromme B, Möller M, Anschüty T, Bethke C and Kisker E 1996 *Phys. Rev. Lett.* **77** 1548
[25] Trzeciecki M, Ney O, Zhang G P and Hübner W 2001 *Adv. Solid State Phys.* **41** 547–55
[26] Hübner W, Bennemann K H and Böhmer K 1994 *Phys. Rev.* B **50** 17597
[27] Grifoni M and Hänggi P 1998 *Phys. Rep.* **304** 229